https://doi.org/10.5194/esd-2020-70
Preprint. Discussion started: 28 September 2020

Earth System Dynamics Discussions

Synchronized spatial shifts of Hadley and Walker circulations

Kyung-Sook Yun[1,2*], Axel Timmermann[1,2], and Malte F. Stuecker[3]

[1]Center for Climate Physics, Institute for Basic Science (IBS), Busan 46241, South Korea
[2]Pusan National University, Busan 46241, South Korea
[3]Department of Oceanography and International Pacific Research Center, School of Ocean and Earth Science and Technology, University of Hawai'i at Mānoa, Honolulu, HI, USA

Correspondence to: Kyung-Sook Yun (kssh@pusan.ac.kr)

Abstract. The El Niño-Southern Oscillation (ENSO) influences the most extensive tropospheric circulation cells on our planet, known as Hadley and Walker circulations. Previous studies have largely focused on the effect of ENSO on the strength of these cells. However, what has remained uncertain is whether interannual sea surface temperature anomalies can also cause synchronized spatial shifts of these circulations. Here, by examining the spatio-temporal relationship between Hadley and Walker cells in observations and climate model experiments, we demonstrate that the seasonally evolving warm pool SST anomalies in the decay phase of an El Niño event generate a meridionally asymmetric Walker circulation response, which couples the zonal and meridional atmospheric overturning circulations. This process, which can be characterized as a phase-synchronized spatial shift in Walker and Hadley cells, is accompanied by cross-equatorial northwesterly low-level flow that diverges from an area of anomalous drying in the western North Pacific and converges towards a region with anomalous moistening in the southern central Pacific. Our results show that the SST-induced concurrent spatial shifts of the two circulations are climatically relevant as they can further amplify extratropical precipitation variability on interannual timescales.

1 Introduction

Changes in the zonal Walker cell (WC; tropical-mean zonal cell) and the meridional Hadley Cell (HC; zonal-mean meridional cell) are known to cause major climate disruptions across our planet. Because of their considerable impacts on various regional climates and extreme events, such as heat waves (Garcia-Herrera et al., 2010), tropical cyclones (Wu et al., 2018), sea level rise in the western Pacific (Timmermann et al., 2010), droughts (Dai, 2011;Lau and Kim, 2015), and regional monsoon variability (Kumar et al., 1999;Bollasina et al., 2011), the variations in the strength and position of WC and HC have been examined extensively across a wide range of timescales. It has been shown that changes in the strength of the WC are connected to those of the HC, in part due to the shared ascending branch of zonal and meridional overturning cells (Vecchi and Soden, 2007;England et al., 2014;Liu and Zhou, 2017;Ma et al., 2018;Klein et al., 1999). On interannual timescales, the co-variability between WC and HC strengths is tied to the El Niño/Southern Oscillation (ENSO) driven sea surface temperature (SST)

https://doi.org/10.5194/esd-2020-70
Preprint. Discussion started: 28 September 2020


Earth System Dynamics Discussions

gradients along the equator, associated with uneven spatial distribution of tropical convection (Oort and Yienger, 1996;Klein et al., 1999;Minobe, 2004). However, observational analyses suggest more complicated relationships, that cannot be fully explained by peak ENSO dynamics alone (Clarke and Lebedev, 1996;Mitas and Clement, 2005;Tanaka et al., 2005;Ma and Zhou, 2016).

In general, these two large-scale circulations can change independently from each, either in terms of their strength or their geographical position. Nevertheless, the coupling of the WC and HC variability has been mostly examined in terms of strength changes during major El Niño and La Niña winters: e.g., during El Niño events, there is a weakening of the WC and strengthening of the HC (Ma and Li, 2008;Bayr et al., 2014;Guo and Tan, 2018;Minobe, 2004;Klein et al., 1999) (also see Supplementary text, Fig. S1, and Table S1). Potential synchronized shifts in their positions have not been fully considered so far. Here we address the question whether and under what conditions WC and HC can also experience concurrent shifts in their geographic positions? We further investigate whether these two dominant atmospheric circulation cells are coupled in the absence of tropical ENSO-related SST anomalies. To address these questions, we conduct a comprehensive analysis of the dynamical coupling between HC and WC using observational data and a series of SST-forced atmospheric general circulation model (AGCM) simulations. We will focus on two important degrees of freedom that characterize variations of these circulations - their strength and spatial position.

2 Data and Method

2.1 Observation

We used the monthly reanalysis circulation dataset from European Centre for Medium-Range Weather Forecasts (ECMWF) interim (ERAI) data from 1979 to 2017 (Dee et al., 2011). In addition, the monthly SST and precipitation data are obtained from the extended reconstruction of global SST (ERSSTv5) since 1854 (Smith et al., 2008) and Global Precipitation Climatology project (GPCP) version 2.3 from 1979 to 2017 (Adler et al., 2003), and Climatic Research Unit (CRU) TS4.03 land precipitation from 1901 to 2017 (Harris et al., 2014), respectively. The monthly anomalies for 1979-2017 were calculated by removing the seasonal cycle and linear trend coefficient during the analysis period. The ENSO variability was identified as Niño3 SST anomalies averaged over the tropical eastern Pacific [5°S-5°N, 150°W-90°W].

2.2 AMIP and CMIP models

We used 40 AGCM simulations from the forced AGCM Intercomparison Projection (AMIP): 19 model runs are part of the Coupled Model Inter-comparison Project (CMIP) Phase 5 (Taylor et al., 2012) and 21 models are part of Phase 6 (Eyring et al., 2016) (i.e., AMIP5 and AMIP6; Supplementary Tables S2 and S3). The AMIP simulations were forced by the observed SST and sea ice concentrations during 1979-2008 for AMIP5 and during 1979-2014 for AMIP6. The AMIP multi-model ensemble (MME) represents the SST-forced variability only compared to a mixed signal of SST-forced variability and unforced

https://doi.org/10.5194/esd-2020-70
Preprint. Discussion started: 28 September 2020


Earth System Dynamics Discussions

atmospheric noise that is present in the observations and individual AMIP simulations. Additionally, we analyzed a 40 multi-model result of CMIP5 historical simulations covering the industrial period from 1900-2005 (see (Taylor et al., 2012) for detail). Only one ensemble member (r1i1p1) was used for each model. All observation and MME data were interpolated to a regular 2.5° × 2.5° horizontal grid before the analyses.

2.3 WC and HC variability

We calculated the monthly mass stream function (MSF) anomalies on the three-dimensional atmospheric circulation to describe the WC and HC circulations:

$$\psi_{WC}(x,z,t) = \frac{2\pi a}{g}\int_{p}^{p_s} u_D\, dp \quad , \tag{1}$$

$$\psi_{HC}(y,z,t) = \frac{2\pi a\cos\phi}{g}\int_{p}^{p_s} [v]\, dp \quad , \tag{2}$$

Following previous work (Yu and Zwiers, 2010), the tropical zonal circulation (ψ_{WC}) is expressed as the divergent component (u_D) of zonal wind averaged over the tropics [5°S-5°N] (zonal mass-stream function). The tropical meridional circulation (ψ_{HC}) is the zonally averaged meridional mass-stream function. Next, an Empirical Orthogonal Function (EOF) analysis of monthly MSF anomalies was used to characterize the dominant modes of the tropical atmospheric mass flux variability. For fair comparison between observations and simulations, the MSF fields in every single model were projected onto the EOF pattern derived from the observations to generate PC time series for the simulated WC and HC variability. The inter-annual component of variability was calculated by applying a 10-point Butterworth band-pass filter with 1.5- year (18-months) and 10-year cutoffs.

2.4 Phase synchronization in WC and HC variabilities

To examine the phase synchronization of the large-scale circulation, we calculate the complex analytical signal ($\hat{T}(t)$) using the Hilbert transform. The amplitude and phase of the PC time series can be obtained from $\hat{T}(t)$, based on a Cartesian to polar coordinate transform (e.g., Stein et al., 2014):

$$\alpha(t) = \sqrt{Re(\hat{T}(t))^2 + Im(\hat{T}(t))^2} \quad \text{and} \quad \Phi(t) = Arg\frac{Im(\hat{T}(t))}{Re(\hat{T}(t))}, \tag{3}$$

The generalized phase difference has the following expression:

$$\Delta\Phi(t) = \Phi_{WC}(t) - \Phi_{HC}(t), \tag{4}$$

where $\Phi_{WC}(t)$ and $\Phi_{HC}(t)$ indicate the phase of the WC and HC PC time series respectively. If the absolute tendency of the phase difference (i.e., $|\frac{d(\Delta\Phi(t))}{dt}|$) is close to zero, then $\Phi_{WC}(t)$ and $\Phi_{HC}(t)$ are synchronized. Thus, we define that the

https://doi.org/10.5194/esd-2020-70
Preprint. Discussion started: 28 September 2020


Earth System Dynamics Discussions Open Access EGU

phases of the WC and HC shift modes are synchronized when the absolute tendency of a smoothed (i.e., 7-month running mean) phase difference is less than 0.3.

3 Result

3.1 Phase synchronized spatial shifts of Walker and Hadley circulations

First, we conduct an EOF analyses of estimates of the monthly MSF anomalies, obtained from atmospheric reanalysis data covering the period 1979-2017. In addition to their co-varying strength (characterized by EOF1 for WC (WC1) and EOF2 for HC (HC2) – shown in Supplementary Fig. 1) that has been discussed extensively in previous studies (Ma and Li, 2008;Bayr et al., 2014;Guo and Tan, 2018;Minobe, 2004), we find that EOF2 for WC (WC2) and EOF1 for HC (HC1) are related to each other (correlation coefficient CC ~ 0.49, Fig, 1a-c). Compared to the climatological circulation pattern (contours in Fig. 1a-b) of WC and HC, WC1 and HC1 describe zonal and meridional shifts occurring over the shared rising branch of the two circulations (shading in Fig. 1a-b) over the Western Pacific Warm Pool. These anomalies characterize an eastward shift of the WC and an equatorially asymmetric clockwise HC that is often referred to as cross-equatorial anomalous HC (Supplementary Table S1 also clearly supports the co-varying zonal and meridional changes in WC and HC variability).

We next explore the relationship between ENSO and the co-varying spatial shifts of the WC and HC (Fig. 1c and e). The very low instantaneous correlation coefficients between the Principal Components (PCs) of WC2 and Niño3 anomalies (CC ~ 0.06 for WC2-Niño3; CC ~ 0.2 for HC1-Niño3) indicate that the peak ENSO dynamics alone cannot explain the synchronized spatial shifts in these two circulations. This stands in sharp contrast with the ENSO-driven co-varying strength (CC ~ 0.91 for WC1-Niño3; CC ~ 0.87 for HC2-Niño3; see also Supplementary Fig. S1c) that has been highlighted previously. Despite the fact that there no linear relationship between ENSO and the co-varying spatial circulation shifts, there is still a pronounced statistically significant relationship between WC2 and HC1 variability (see Fig. 1d; CC ~ 0.66 significant at 99% confidence level) in a 40 member MME of SST-forced AMIP experiments. This raises the question which type of seasonally-modulated SST dynamics is responsible for the synchronized spatial shifts in WC and HC. It is worth noting that the WC2-HC1 linkage breaks down when the SST-forced MME component is subtracted from the PCs of individual AMIP runs (i.e., PC differences between individual AMIP simulations and the MME; Supplementary Fig. S2).

This discrepancy calls for two important aspects of ENSO to be considered: one is the peak ENSO variability (which occurs in boreal winter); the other are the seasonally modulated dynamics of ENSO, i.e., the combination mode between ENSO and the Indo-Pacific warm pool SST annual cycle (C-mode; which peaks in boreal spring) (Stuecker et al., 2013;Stuecker et al., 2015). In fact, the "Walker and Hadley shift modes" are statistically significantly connected to Niño3 during boreal spring (CC ~ 0.55 for WC2-Niño3; CC ~ 0.52 for HC1-Niño3; Supplementary Fig. S3). We hypothesize here that the seasonally evolving warm pool SST anomalies after the peak ENSO phase (i.e., C-mode) serve as a pacemaker linking the phase-synchronized spatial shifts in WC and HC variability. The WC2-regressed SSTA pattern (bottom in Fig. 1a) also bears

https://doi.org/10.5194/esd-2020-70
Preprint. Discussion started: 28 September 2020

Earth System Dynamics
Discussions
Open Access
EGU

resemblance with the previously suggested C-mode generated SST dipole pattern with anomalous warming in the Southern Indian Ocean (SIO) and anomalous cooling in the WNP (Stuecker et al., 2015;Zhang et al., 2016). This suggests that the Walker and Hadley shift modes are linked via nonlinear C-mode dynamics, rather than the common ENSO indices (such as Niño3) that instead describe peak boreal winter ENSO variability and the associated Walker and Hadley strength modes (Supplementary Fig. S1).

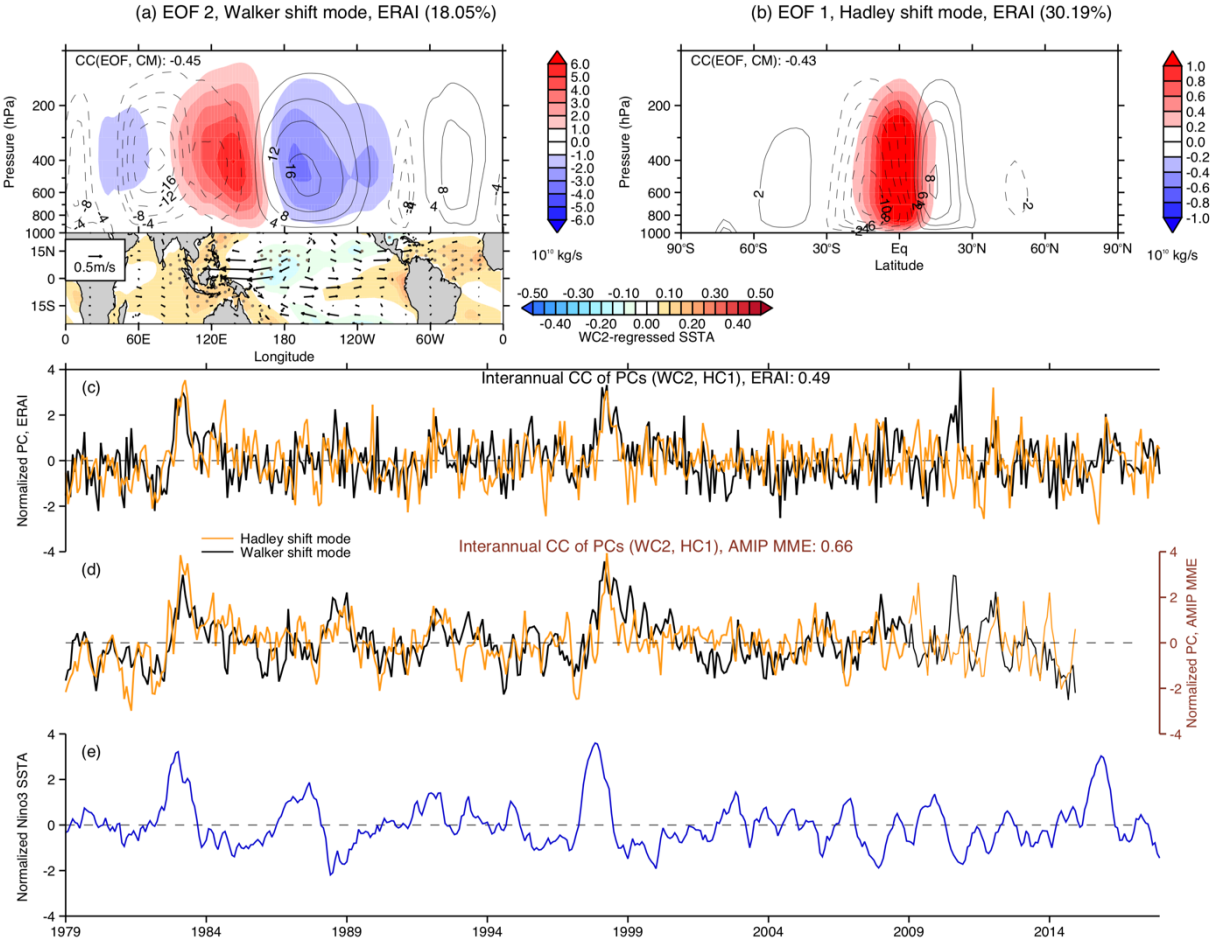

Figure 1: Phase synchronized spatial shifts of the Walker and Hadley circulations. (a-b) The dominant patterns of the shift modes (i.e., EOF2 for Walker and EOF1 for Hadley; denoted by shading) for (a) Walker circulation (WC) and (b) Hadley circulation (HC) variability. The WC and HC are identified as (a) tropical (5°S-5°N) averaged mass stream function (MSF) anomalies and (b) zonally averaged MSF anomalies, obtained from the monthly ERA interim (ERAI) data during the period 1979-2017. The contours show the climatological mean (CM) of the MSF for the circulations. The pattern correlation coefficients (CCs) between EOF and CM are also displayed in (a-b). The SST and 850hPa wind anomaly patterns regressed against the WC2 principal component (PC) are displayed as a bottom inset in (a). (c-d) The normalized PC time series of the shift modes (i.e., WC2 and HC1), derived from (c) ERAI and (d) the multi-model ensemble (MME) average

https://doi.org/10.5194/esd-2020-70
Preprint. Discussion started: 28 September 2020


Earth System Dynamics Discussions

for 40 AMIP models (1979-2008 for 19 AMIP5 and 1979-014 for 21 AMIP6 models). (e) The normalized Niño3 SST anomaly (ERSSTv5) time evolution.

3.2 SST-forced variability of Walker and Hadley circulations

To further study this synchronization, we first calculate the generalized phase difference between WC2 and HC1 variabilities (i.e., $\Delta\Phi(t) = \Phi 1 - \Phi 2$), using the complex analytical signal of the respective principal components WC PC2 and HC PC1. The analytical signal approach embeds a timeseries into a complex space by adding the original timeseries with the Hilbert transform of this timeseries times the imaginary number (Pikovsky et al., 2000;Stein et al., 2014;Rosenblum et al., 1998;Rosenblum, 2000;Tass et al., 1998). The phase difference between WC2 PC and HC1 PC (Fig. 2a) shows periods of near constant phase difference. Constant phase differences, which occur more frequently than expected by randomness, are indicative of the emergence of *phase synchronization* between WC and HC shift modes. Phase synchronization, which requires nonlinear dynamics, characterizes a specific type of cooperative, organized oscillatory behavior between two fluctuating systems. When the absolute tendency of the phase difference (i.e., $|d(\Delta\Phi(t))/dt|$) in our calculations is less than 0.3 degrees/month (Fig. 2a), we refer to the period as a phase-synchronized period. During these periods the phases of two signals are not drifting apart randomly but are bounded by the underlying nonlinear interactions.

We next examine the question whether the synchronization of "Walker and Hadley shift modes" can in principle be driven by random atmospheric stochastic variability, or if SST-forced variability is a prerequisite. The SST-forced AMIP MME shows more frequent phase-synchronized (PSYN) months than the observations (Fig. 2a), exhibiting the effects of both SST forcing and atmospheric noise: There are four long-lasting (greater than 6 months) PSYN events in the observations but eight events in the AMIP MME (see Figs. 2d and 2e). The WC-HC phase synchronization is particularly prominent during the two extreme El Niño events (1982-1893 and 1997-1998) that have much longer PSYN periods (exceeding 1-year) in both observations and the AMIP MME. An interesting point is that the WC-HC phase difference shows a decadal change after 2000 in both observations and the AMIP MME. This may be a consequence of the Pacific WC intensification amplified by Atlantic warming (England et al., 2014;McGregor et al., 2014). Further exploration of the underlying physical mechanisms is, however, beyond the scope of this study.

To further examine the relative effect of random atmospheric noise and SST-forced variabilities on the WC-HC synchronization, we generate pseudo-PCs by randomly shuffling the PCs for both the observations and the AMIP MME and repeating this 10 times. A comparison of the phase difference tendencies using the original PCs (pink dots in Fig. 2b, c)) and of the pseudo-PCs (sky blue dots) reveals that in case of extreme El Niño events (Niño3 > 1.5 standard deviations (SDs); denoted by gray shading), the phase synchronization (i.e., $|d(\Delta\Phi(t))/dt| < 0.3$) of the original PCs is clearly distinguishable from the pseudo-PCs that have randomized phases: The occurrence probability for phase synchronization (i.e., the ratio of the PSYN number compared to the number in the gray shaded area) is ~ 83% for the observations and 96% for the AMIP MME, whereas the ratio for the pseudo-PCs (sky blue dots) is only ~33% in the observations and 39% in the AMIP MME (Figs. 2b

https://doi.org/10.5194/esd-2020-70
Preprint. Discussion started: 28 September 2020

Earth System Dynamics
Discussions
Open Access
EGU

and 2c). The PSYN probability from pseudo-PCs in case of extreme El Niño events is almost the same to the probability in entire samples (~ 35%). The randomized pseudo-PCs also cannot reproduce the long-lasting duration periods of PSYN (see blue bar in Figs. 2d and 2e). Consequently, this result indicates that even though the temporal correlation between all month Niño3.4 SSTA and PC2 WC and PC1 HC is marginal, eastern equatorial Pacific SST forcing still leads to an increasing probability for WC-HC phase synchronization and its long-lasting duration. This discrepancy can be explained by the fact that correlations emphasize amplitude relationships and are less sensitive to seasonally modulated coupling which is induced by the phase-synchronization mechanism.

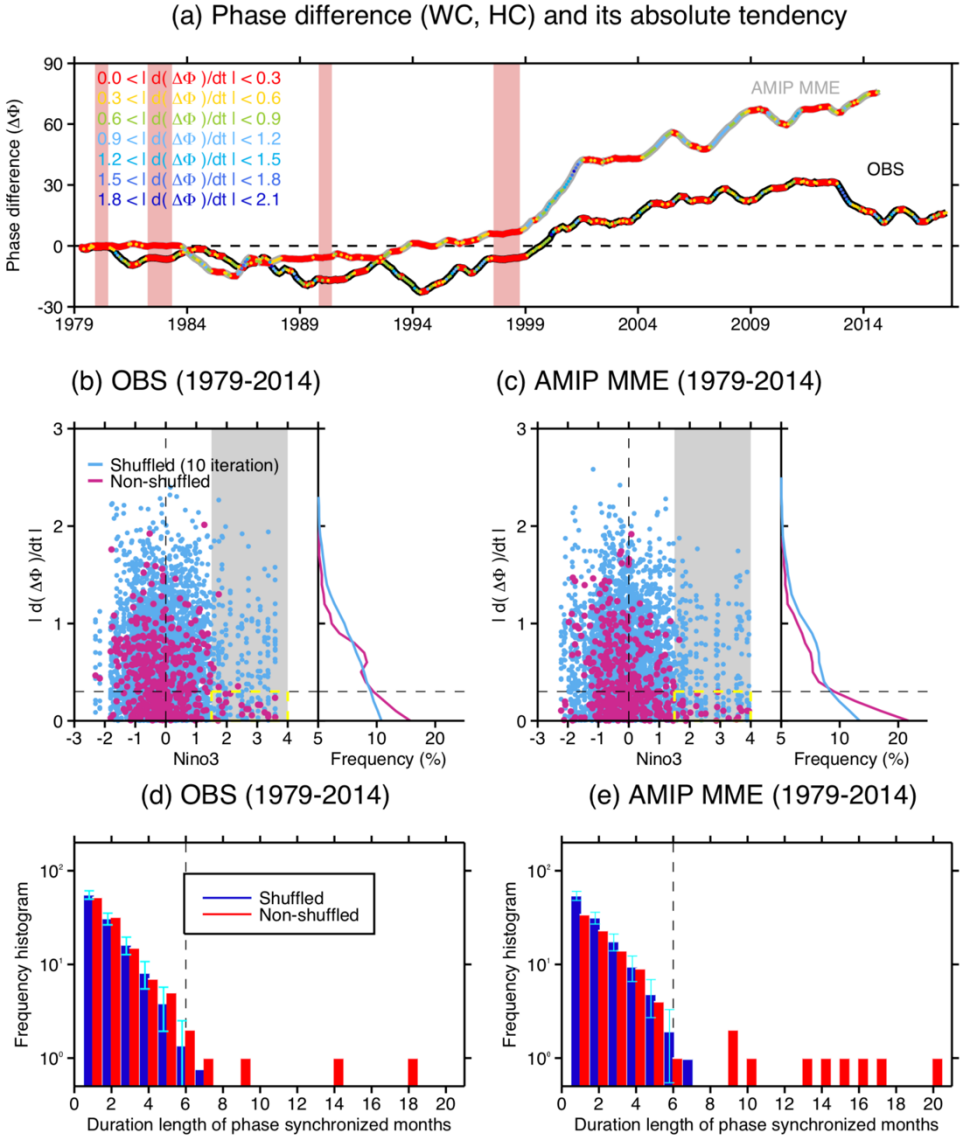

https://doi.org/10.5194/esd-2020-70
Preprint. Discussion started: 28 September 2020

Earth System Dynamics Discussions

Figure 2: SST-forced phase synchronized spatial shifts of the HC and WC. (a) The smoothed (i.e, 7-month running mean) phase difference between PC time series of WC2 and HC1 (thick line) and its absolute tendency (colored dots), obtained from the ERAI observational data (1979-2017; black) and AMIP MME (1979-2014; gray). Here, the phase is calculated from the analytical signal of the PCs using the Hilbert transform (see Method section for detail). The phase synchronized (PSYN) months are measured by the criterion that the absolute tendency of phase difference is less than 0.3 °/month. The red vertically shaded zone indicates PSYN periods that are identical for both observations and the AMIP MME. (b-c) The absolute tendency of WC-HC phase difference as a function of Niño3 SST anomaly (pink), obtained from the (b) observations and (c) AMIP MME. Sky blue dots indicate tendencies calculated from the randomly shuffled PCs. The frequency histogram of the absolute tendency of the WC-HC phase difference is also vertically plotted in each right inset. (d-e) Frequency histogram (red bar) for duration length of PSYN months, based on PC variability from the (d) observations and (e) AMIP MME. To test the effect of randomly perturbed variability on the PSYN, the original data were shuffled 1000 times and the mean and standard deviation (SD) within duration lengths calculated from the 1000 sample are shown by blue bars and the vertical error bars respectively.

Figure 3a clearly shows the statistically significant co-variability between observed time series of WC-HC PCs and the C-mode (which is defined here as $Niño3 \times cos(\omega_a(t) - \varphi)$; where $\omega_a(t)$ is angular frequency of the annual cycle and and φ is a one-month phase shift; Ref (Stuecker et al., 2013)) (CC ~ 0.61 and 0.58 on inter-annual timescales). In addition to the C-mode index, we also consider a SST index representing C-mode dynamics, which is calculated from the SST gradient between the SIO [20°S-5°S, 90°E-120°E] and the WNP [0°-15°N, 140°E-170°E] (i.e., SSTgrad; ΔSST(SIO, WNP)), as shown by the WC2-regressed SST pattern in Fig. 1a. However, different from the winter-maximum El Niño variability, the SSTgrad variability peaks in boreal spring (Supplementary Fig. S4). The largest variability in both WC and HC shift modes also appears in spring (i.e., February-March-April; FMA) (Figs. 3b-3g). This springtime seasonal preference is evident within the SSTgrad (or C-mode) index, resulting in a statistically significant relationship between SSTgrad and WC-HC coupling in both observations and the AMIP MME (Figs. 3d and 3g).

https://doi.org/10.5194/esd-2020-70
Preprint. Discussion started: 28 September 2020

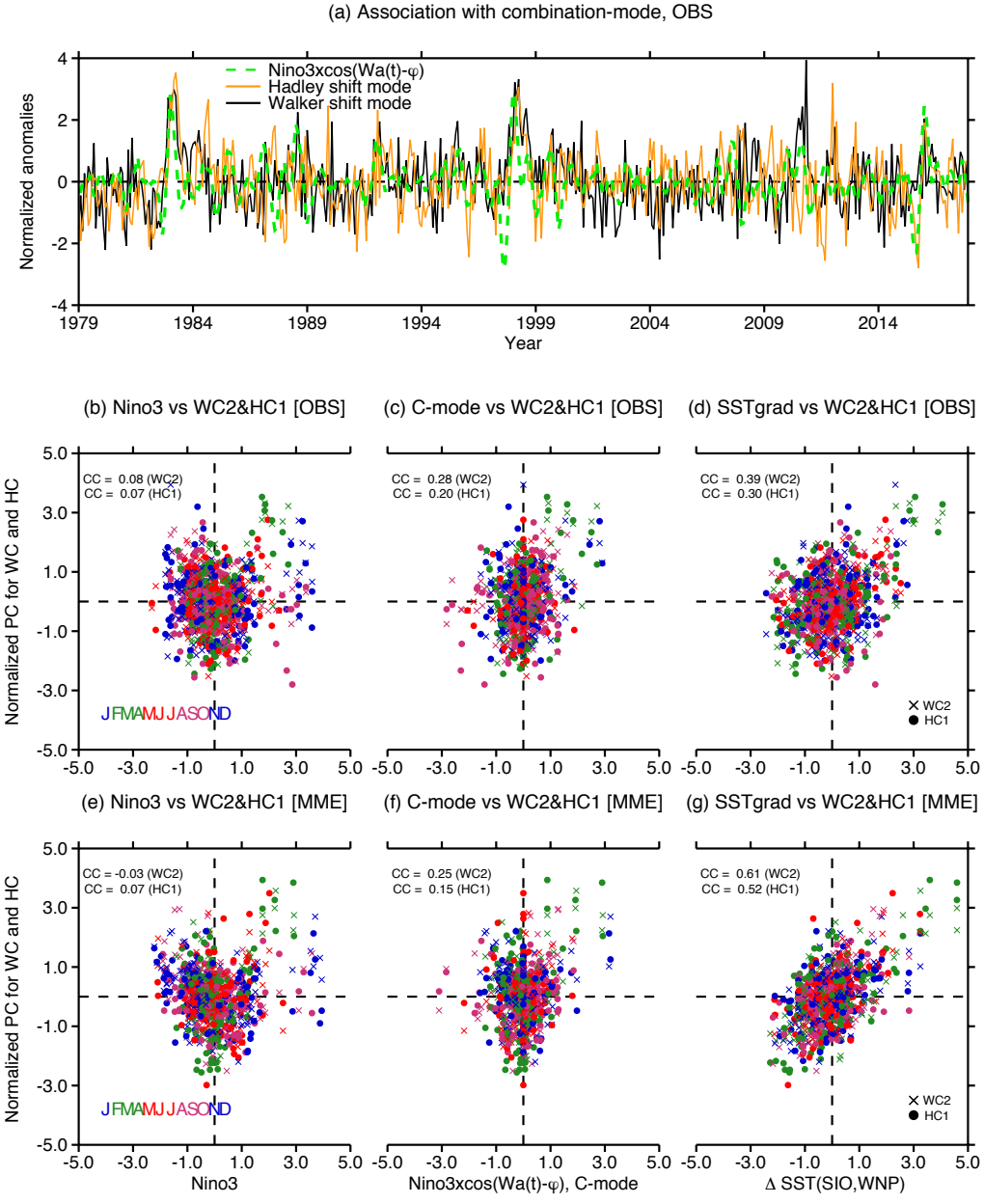

Figure 3: Seasonal dependency of phase synchronized spatial shifts of the HC and WC. (a) The normalized PC time series of the shift modes (i.e., WC2 & HC1) and the combination mode (Stuecker et al., 2013; dashed green line). (b-g) Scatter plot of normalized time series for SST anomalies (x-axis) versus PCs of WC2 (x symbol) and HC1 (y-axis), obtained from the observations (1979-2017; b-d) and the AMIP MME (1979-2014; e-g): (b, e) Niño3, (c, f) combination mode, and (d, g) SST gradient between Southern Indian Ocean [20°S-5°S, 90°E-120°E] and western North Pacific [0°-15°N, 140°E-170°E] (SSTgrad). Each season is displayed in different colors.

https://doi.org/10.5194/esd-2020-70
Preprint. Discussion started: 28 September 2020

Earth System Dynamics Discussions
Open Access
EGU

215

3.3 Global pattern and impact of phase synchronized spatial shifts

Our results suggest that the spring SSTgrad anomalies that occur after the El Niño winter peak phase (Stuecker et al., 2015;Zhang et al., 2016) play an important role for the phase synchronization of WC and HC shift modes. We further examine a physical mechanism for the WC-HC phase synchronized spatial shifts by exploring the global climate patterns that occur during springtime phase-synchronized periods in WC and HC variability (Fig. 4; composite when $|d(\Delta\Phi(t))/dt| < 0.3$ °/month and FMA[1] Niño3 > 1.5SD). A key feature is that the center of low-level divergence and drying is located over the off-equatorial WNP region, whereas the center of convergence and moistening is situated in the off-equatorial southern central Pacific (corresponding to the C-mode pattern discussed in previous studies (Stuecker et al., 2015;Stuecker et al., 2013)). This equatorially asymmetric circulation pattern is considerably different from the equatorially symmetric pattern derived from the wintertime PSYN composite (see Supplementary Fig. 5). The meridionally asymmetric WC can be linked to the HC, along with cross-equatorial northwesterly flow. A general agreement between the observation-based and AMIP MME-based patterns also reflects that the SST-forced variability acts to modulate the phase synchronization of the WC-HC shift modes.

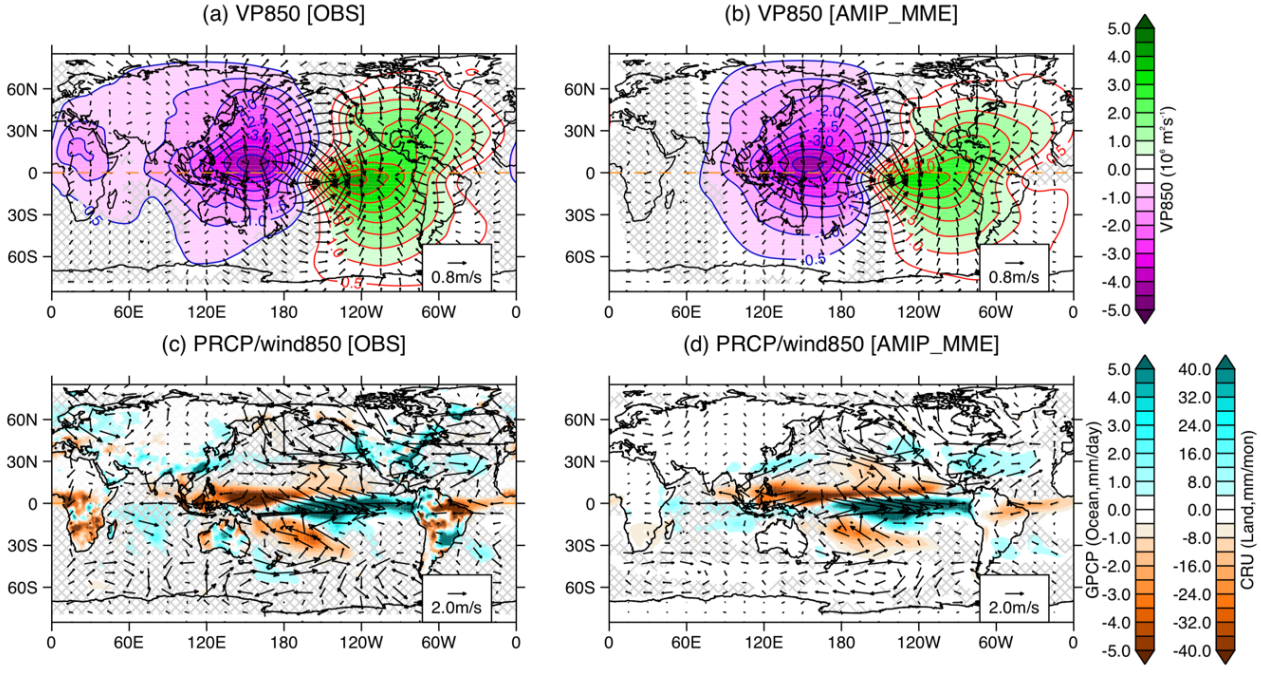

Figure 4: Global pattern of phase synchronized spatial shifts of HC and WC. Composite anomalies during PSYN months (i.e., the absolute tendency of phase difference is less than 0.3) with February-March-April (FMA[1]) extreme El Niño (FMA[1] Niño3 > 1.5SD), obtained from the observations (left column) and the AMIP MME (right column): (a, b) 850 hPa velocity potential (VP850) anomaly; (c-d)

https://doi.org/10.5194/esd-2020-70
Preprint. Discussion started: 28 September 2020


Earth System Dynamics Discussions

precipitation (GPCP for ocean and CRU for land; shading) and 850hPa wind (vector) anomaly. The hatching shows the area where the difference is statistically insignificant at the 95% confidence level.

We emphasize that the simulated ENSO SST anomaly amplitudes in coupled models of the CMIP5 are correlated with the probability of phase synchronization between the WC and HC shift modes (Supplementary Fig. S6). The models exhibiting large ENSO variability can initiate strong teleconnections through the atmospheric bridge process, thus likely leading to the phase synchronized zonal and meridional shifts of the WC and HC, respectively (see Supplementary Fig. S7). An underlying cause could be the strong meridional asymmetry of the warm pool climatological SST and zonal winds (Supplementary Fig. S8) and C-mode associated extreme shifts of the South Pacific Convergence Zone (SPCZ) shifts (McGregor et al., 2012). We further hypothesize that stronger phase synchronization of the WC-HC shift modes can generate larger global precipitation responses, regardless of the ENSO amplitude. To illustrate this, we use the individual 40 AMIP simulations that have identical ENSO SST amplitude prescribed as their boundary forcing but exhibit different strengths of WC2-HC1 phase synchronization. The strong PSYN models and weak PSYN models are thus classified as a function of their strength of WC2-HC1 phase synchronization, where this strength is measured by the (inter-annual) correlation coefficient between WC2 and HC1 PC variations in the individual AMIPs (see Supplementary Tables S2 and S3 for chosen model groups).

By comparing the strong El Niño (i.e., 1982/83 and 1997/1998) composite averaged for eight strong PSYN models with that averaged for eight weak PSYN models (Fig. 5), we see that the models with a strong coupling between the HC and WC shift modes generate a prominent springtime (FMA) asymmetry between WNP divergence and southern eastern Pacific convergence. Accordingly, there are increased precipitation anomalies in the extratropical East Asia (EA) and South America (SA) regions (Figs. 5c and 5d). The inter-model comparison between individual strong and weak PSYN models shows a clear difference in both precipitation anomalies over EA and SA and the meridional displacement between the WNP divergence and southern eastern Pacific convergence, which is only statistically significant during boreal spring but not during boreal winter (Fig. 5e). This reflects the pronounced impact of WC-HC phase-synchronized spatial shifts on extratropical precipitation variability.

https://doi.org/10.5194/esd-2020-70
Preprint. Discussion started: 28 September 2020

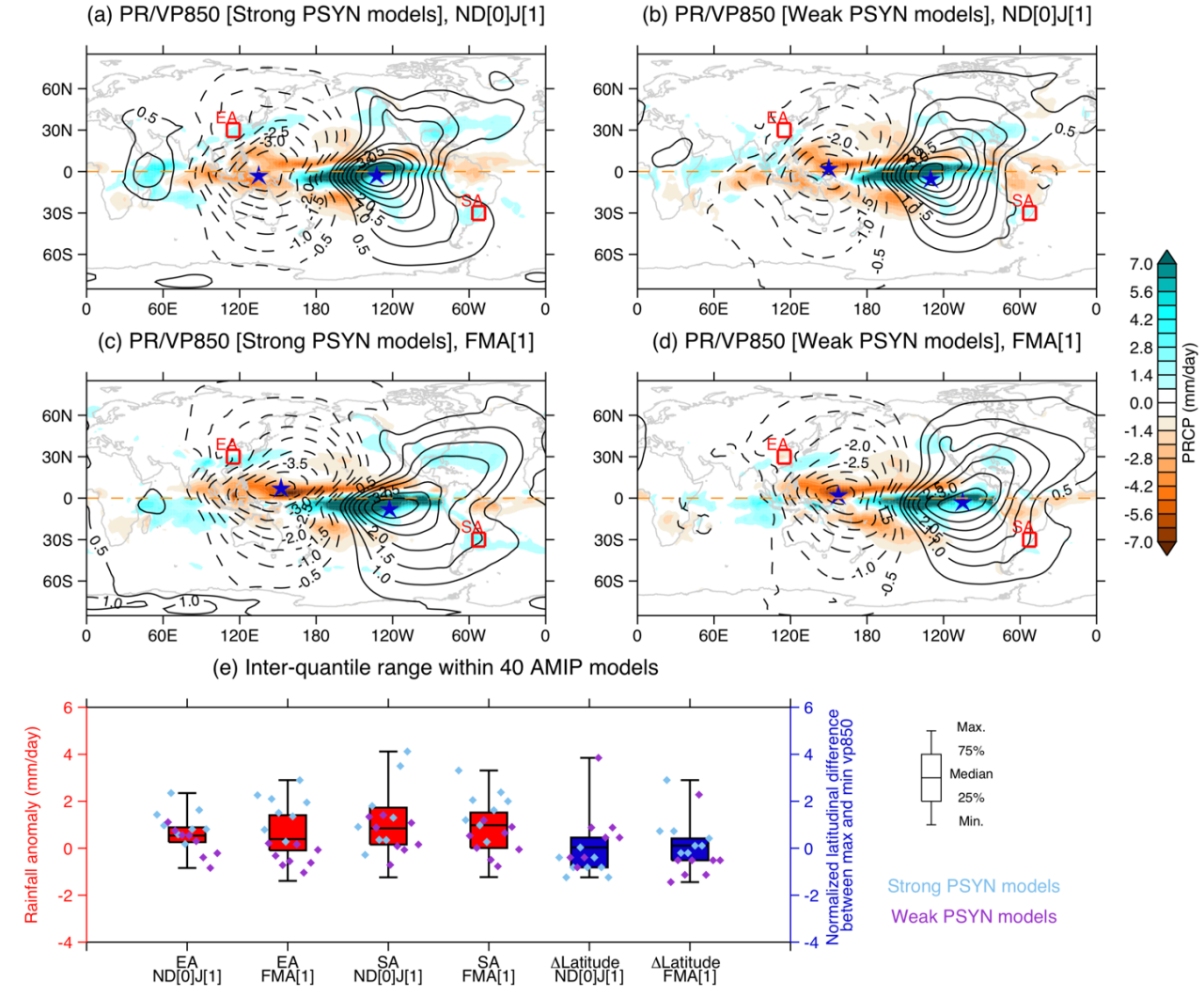

Figure 5: Impact of phase synchronized spatial shifts of the HC and WC on global precipitation. (a-b) The November-December[0]-January[1] and (c-d) February-March-April (FMA[1]) extreme El Niño (i.e., 1982/1983 and 1997/1998) composite anomaly of precipitation (shading) and VP850 (contours) obtained from the (a, c) 8 strong PSYN models in the AMIP simulations and (b, d) 8 weak PSYN models. The blue star symbol indicates the positions of maximum and minimum VP850 anomalies. Here, the strong PSYN and weak PSYN model groups are categorized according to inter-annual correlation coefficients between WC2 and HC1 within 19 AMIP5 and 21 AMIP6 models, respectively (see Supplementary Tables 2 and 3). (e) Inter-quantile range of area-averaged precipitation anomalies (red filled box) and normalized difference between the latitudes at maximum and minimum VP850 (blue filled box) within the 40 AMIP simulations: The domain for the area-average is denoted by red boxes in (a-d) over the East Asia [EA; 25°N-35°N, 110°E-120°E] and South America [SA; 35°S-25°S, 57.5°W-47.5°W]. The strong PSYN (sky blue) and weak PSYN (purple) models are also shown in individual diamond symbols.

https://doi.org/10.5194/esd-2020-70
Preprint. Discussion started: 28 September 2020


Earth System Dynamics Discussions
Open Access
EGU

4 Discussion and Conclusion

Here we examined the intricate coupling between the WC and HC. In addition to a well-known ENSO driven coupling of WC and HC variability amplitude, our study shows that these two circulations can also shift their positions in a synchronized manner. Focusing on the zonal and meridional displacements of both circulations, using observational datasets and the AMIP MME simulations, our analysis revealed that the seasonally evolving springtime warm pool SST anomalies after an El Niño winter can produce a meridionally asymmetric WC and anomalous cross-equatorial flow, thus connecting the zonal WC and meridional HC. This feature is reminiscent of the atmospheric ENSO C-mode. Coherent WC-HC shifts have pronounced influences on precipitation, as well as wind and sea-level patterns in both tropical and extratropical regions.

An important finding of our study is that the phase-synchronization is only present for extreme El Niño events, however not for La Niña, indicating an important nonlinearity of the tropical climate system. In addition, potential asymmetric heat capacitor effects of both the Indian and Atlantic Oceans, that tend to be more pronounced during El Niño compared to La Niña (Ohba and Watanabe, 2012;An and Kim, 2018) may further affect the phase synchronization properties discussed here. We found that the meridionally asymmetric response for phase synchronization of the WC-HC shift mode is quite different from the meridonally symmetric response associated with the strength-related WC-HC modes (Supplementary Figs. S9 and S10). Our analysis also highlights the fact that the analysis of phase-relationships (Rosenblum and Pikovsky, 2003) between modes of climate variability can reveal important new insights into their physical coupling mechanisms, that are less apparent in amplitude space (as described for instance by temporal correlation coefficients).

https://doi.org/10.5194/esd-2020-70
Preprint. Discussion started: 28 September 2020

Earth System Dynamics Discussions

Code and Data availability

Observation data for this research are available at (1) ECMWF website (https://www.ecmwf.int/en/forecasts/dataset/ecmwf-reanalysis-interim) for ERA-Interim reanalysis data, (2) NCDC (https://www.ncdc.noaa.gov/data-access/marineocean-data/extended-reconstructed-sea-surface-temperature-ersst-v5) for ERSST v5, and (3) ESRL (https://www.esrl.noaa.gov/psd/data/ gridded/data.gpcp.html) for GPCP v2.3, and (4) the website (https://crudata.uea.ac.uk/cru/data/hrg/ cru_ts_4.03/) for CRU TS4.03.The model data for both AMIP and CMIP are also available at a publicly accessible CMIP5 website (https://esgf-node.llnl.gov/search/cmip5/) and CMIP6 website (https://esgf-node.llnl.gov/search/cmip6/).

Author Contributions

AT and K-SY designed the study. K-SY wrote the initial manuscript draft and produced all figures. K-SY, AT, and MFS contributed to the interpretation of the results and to the improvement of the manuscript.

Acknowledgements

This study was supported by the Institute for Basic Science (project code IBS-R028-D1). This is IPRC publication X and SOEST contribution Y.

Competing Interests

The authors declare that they have no competing financial interests.

References

Adler, R. F., Huffman, G. J., Chang, A., Ferraro, R., Xie, P. P., Janowiak, J., Rudolf, B., Schneider, U., Curtis, S., Bolvin, D., Gruber, A., Susskind, J., Arkin, P., and Nelkin, E.: The version-2 global precipitation climatology project (GPCP) monthly precipitation analysis (1979-present), J Hydrometeorol, 4, 1147-1167, 10.1175/1525-7541(2003)004<1147:Tvgpcp>2.0.Co;2, 2003.

An, S.-I., and Kim, J.-W.: ENSO Transition Asymmetry: Internal and External Causes and Intermodel Diversity, Geophysical Research Letters, 45, 5095-5104, 10.1029/2018gl078476, 2018.

https://doi.org/10.5194/esd-2020-70
Preprint. Discussion started: 28 September 2020

Bayr, T., Dommenget, D., Martin, T., and Power, S. B.: The eastward shift of the Walker Circulation in response to global warming and its relationship to ENSO variability, Climate Dynamics, 43, 2747-2763, 10.1007/s00382-014-2091-y, 2014.

Bollasina, M. A., Ming, Y., and Ramaswamy, V.: Anthropogenic Aerosols and the Weakening of the South Asian Summer Monsoon, Science, 334, 502-505, 10.1126/science.1204994, 2011.

Clarke, A. J., and Lebedev, A.: Long-term changes in the equatorial Pacific trade winds, Journal of Climate, 9, 1020-1029, Doi 10.1175/1520-0442(1996)009<1020:Ltcite>2.0.Co;2, 1996.

Dai, A. G.: Drought under global warming: a review, Wiley Interdisciplinary Reviews-Climate Change, 2, 45-65, 10.1002/wcc.81, 2011.

Dee, D. P., Uppala, S. M., Simmons, A. J., Berrisford, P., Poli, P., Kobayashi, S., Andrae, U., Balmaseda, M. A., Balsamo, G., Bauer, P., Bechtold, P., Beljaars, A. C. M., van de Berg, L., Bidlot, J., Bormann, N., Delsol, C., Dragani, R., Fuentes, M., Geer, A. J., Haimberger, L., Healy, S. B., Hersbach, H., Hólm, E. V., Isaksen, L., Kållberg, P., Köhler, M., Matricardi, M., McNally, A. P., Monge-Sanz, B. M., Morcrette, J. J., Park, B. K., Peubey, C., de Rosnay, P., Tavolato, C., Thépaut, J. N., and Vitart, F.: The ERA-Interim reanalysis: configuration and performance of the data assimilation system, Quarterly Journal of the Royal Meteorological Society, 137, 553-597, 10.1002/qj.828, 2011.

England, M. H., McGregor, S., Spence, P., Meehl, G. A., Timmermann, A., Cai, W., Gupta, A. S., McPhaden, M. J., Purich, A., and Santoso, A.: Recent intensification of wind-driven circulation in the Pacific and the ongoing warming hiatus, Nature Climate Change, 4, 222-227, 10.1038/nclimate2106, 2014.

Eyring, V., Bony, S., Meehl, G. A., Senior, C. A., Stevens, B., Stouffer, R. J., and Taylor, K. E.: Overview of the Coupled Model Intercomparison Project Phase 6 (CMIP6) experimental design and organization, Geosci Model Dev, 9, 1937-1958, 10.5194/gmd-9-1937-2016, 2016.

Garcia-Herrera, R., Diaz, J., Trigo, R. M., Luterbacher, J., and Fischer, E. M.: A Review of the European Summer Heat Wave of 2003, Crit Rev Env Sci Tec, 40, 267-306, 10.1080/10643380802238137, 2010.

Guo, Y. P., and Tan, Z. M.: Relationship between El Nino-Southern Oscillation and the Symmetry of the Hadley Circulation: Role of the Sea Surface Temperature Annual Cycle, Journal of Climate, 31, 5319-5332, 10.1175/Jcli-D-17-0788.1, 2018.

Harris, I., Jones, P. D., Osborn, T. J., and Lister, D. H.: Updated high-resolution grids of monthly climatic observations - the CRU TS3.10 Dataset, International Journal of Climatology, 34, 623-642, 10.1002/joc.3711, 2014.

Klein, S. A., Soden, B. J., and Lau, N.-C.: Remote Sea Surface Temperature Variations during ENSO: Evidence for a Tropical Atmospheric Bridge, Journal of Climate, 12, 917-932, 10.1175/1520-0442(1999)012<0917:Rsstvd>2.0.Co;2, 1999.

Kumar, K. K., Rajagopalan, B., and Cane, M. A.: On the weakening relationship between the Indian monsoon and ENSO, Science, 284, 2156-2159, DOI 10.1126/science.284.5423.2156, 1999.

Lau, W. K., and Kim, K. M.: Robust Hadley Circulation changes and increasing global dryness due to CO2 warming from CMIP5 model projections, Proc Natl Acad Sci U S A, 112, 3630-3635, 10.1073/pnas.1418682112, 2015.

Liu, B., and Zhou, T. J.: Atmospheric footprint of the recent warming slowdown, Sci Rep-Uk, 7, 40947, 10.1038/srep40947, 2017.

https://doi.org/10.5194/esd-2020-70
Preprint. Discussion started: 28 September 2020

Ma, J., and Li, J. P.: The principal modes of variability of the boreal winter Hadley cell, Geophysical Research Letters, 35, L01808, 10.1029/2007gl031883, 2008.

Ma, J., Chadwick, R., Seo, K. H., Dong, C. M., Huang, G., Foltz, G. R., and Jiang, J. H.: Responses of the Tropical Atmospheric Circulation to Climate Change and Connection to the Hydrological Cycle, Annu Rev Earth Pl Sc, 46, 549-580, 10.1146/annurev-earth-082517-010102, 2018.

Ma, S., and Zhou, T.: Robust Strengthening and Westward Shift of the Tropical Pacific Walker Circulation during 1979–2012: A Comparison of 7 Sets of Reanalysis Data and 26 CMIP5 Models, Journal of Climate, 29, 3097-3118, 10.1175/jcli-d-15-0398.1, 2016.

McGregor, S., Timmermann, A., Schneider, N., Stuecker, M. F., and England, M. H.: The Effect of the South Pacific Convergence Zone on the Termination of El Niño Events and the Meridional Asymmetry of ENSO, Journal of Climate, 25, 5566-5586, 10.1175/jcli-d-11-00332.1, 2012.

McGregor, S., Timmermann, A., Stuecker, M. F., England, M. H., Merrifield, M., Jin, F.-F., and Chikamoto, Y.: Recent Walker circulation strengthening and Pacific cooling amplified by Atlantic warming, Nature Climate Change, 4, 888-892, 10.1038/nclimate2330, 2014.

Minobe, S.: Year-to-Year Variability in the Hadley and Walker Circulations from NCEP/NCAR Reanalysis Data, in: The Hadley Circulation: Present, Past and Future, edited by: Diaz, H. F., and Bradley, R. S., Springer, Dordrecht, 153-171, 2004.

Mitas, C. M., and Clement, A.: Has the Hadley cell been strengthening in recent decades?, Geophysical Research Letters, 32, L030809, 10.1029/2004gl021765, 2005.

Ohba, M., and Watanabe, M.: Role of the Indo-Pacific Interbasin Coupling in Predicting Asymmetric ENSO Transition and Duration, Journal of Climate, 25, 3321-3335, 10.1175/jcli-d-11-00409.1, 2012.

Oort, A. H., and Yienger, J. J.: Observed interannual variability in the Hadley circulation and its connection to ENSO, Journal of Climate, 9, 2751-2767, Doi 10.1175/1520-0442(1996)009<2751:Oivith>2.0.Co;2, 1996.

Pikovsky, A., Rosenblum, M., and Kurths, J.: Phase synchronization in regular and chaotic systems, International Journal of Bifurcation and Chaos, 10, 2291-2305, 10.1142/s0218127400001481, 2000.

Rosenblum, M.: Synchronization analysis of bivariate time series and its application to medical data, in: Medical Data Analysis, Proceedings, edited by: Brause, R. W., and Hanisch, E., Lecture Notes in Computer Science, 15-16, 2000.

Rosenblum, M., and Pikovsky, A.: Synchronization: from pendulum clocks to chaotic lasers and chemical oscillators, Contemporary Physics, 44, 401-416, 10.1080/00107510310001603129, 2003.

Rosenblum, M. G., Kurths, J., Pikovsky, A., Schafer, C., Tass, P., and Abel, H. H.: Synchronization in noisy systems and cardiorespiratory interaction, Ieee Engineering in Medicine and Biology Magazine, 17, 46-53, 10.1109/51.731320, 1998.

Smith, T. M., Reynolds, R. W., Peterson, T. C., and Lawrimore, J.: Improvements to NOAA's Historical Merged Land–Ocean Surface Temperature Analysis (1880–2006), Journal of Climate, 21, 2283-2296, 10.1175/2007jcli2100.1, 2008.

Stein, K., Timmermann, A., Schneider, N., Jin, F.-F., and Stuecker, M. F.: ENSO Seasonal Synchronization Theory, Journal of Climate, 27, 5285-5310, 10.1175/jcli-d-13-00525.1, 2014.

https://doi.org/10.5194/esd-2020-70
Preprint. Discussion started: 28 September 2020

405 Stuecker, M. F., Timmermann, A., Jin, F.-F., McGregor, S., and Ren, H.-L.: A combination mode of the annual cycle and the El Niño/Southern Oscillation, Nature Geoscience, 6, 540-544, 10.1038/ngeo1826, 2013.

Stuecker, M. F., Jin, F.-F., Timmermann, A., and McGregor, S.: Combination Mode Dynamics of the Anomalous Northwest Pacific Anticyclone, Journal of Climate, 28, 1093-1111, 10.1175/jcli-d-14-00225.1, 2015.

Tanaka, H. L., Ishizaki, N., and Nohara, D.: Intercomparison of the Intensities and Trends of Hadley, Walker and Monsoon
410 Circulations in the Global Warming Projections, Sola, 1, 77-80, 10.2151/sola.2005.021, 2005.

Tass, P., Rosenblum, M. G., Weule, J., Kurths, J., Pikovsky, A., Volkmann, J., Schnitzler, A., and Freund, H. J.: Detection of n : m phase locking from noisy data: Application to magnetoencephalography, Physical Review Letters, 81, 3291-3294, 10.1103/PhysRevLett.81.3291, 1998.

Taylor, K. E., Stouffer, R. J., and Meehl, G. A.: An Overview of Cmip5 and the Experiment Design, Bulletin of the American
415 Meteorological Society, 93, 485-498, 10.1175/Bams-D-11-00094.1, 2012.

Timmermann, A., McGregor, S., and Jin, F. F.: Wind Effects on Past and Future Regional Sea Level Trends in the Southern Indo-Pacific, Journal of Climate, 23, 4429-4437, 10.1175/2010jcli3519.1, 2010.

Vecchi, G. A., and Soden, B. J.: Global Warming and the Weakening of the Tropical Circulation, Journal of Climate, 20, 4316-4340, 10.1175/jcli4258.1, 2007.

420 Wu, L., Zhang, H. J., Chen, J. M., and Feng, T.: Impact of Two Types of El Nino on Tropical Cyclones over the Western North Pacific: Sensitivity to Location and Intensity of Pacific Warming, Journal of Climate, 31, 1725-1742, 10.1175/Jcli-D-17-0298.1, 2018.

Yu, B., and Zwiers, F. W.: Changes in equatorial atmospheric zonal circulations in recent decades, Geophysical Research Letters, 37, L05701, 10.1029/2009gl042071, 2010.

425 Zhang, W., Jin, F.-F., Stuecker, M. F., Wittenberg, A. T., Timmermann, A., Ren, H.-L., Kug, J.-S., Cai, W., and Cane, M.: Unraveling El Niño's impact on the East Asian Monsoon and Yangtze River summer flooding, Geophysical Research Letters, 43, 11,375-311,382, 10.1002/2016gl071190, 2016.

430